Fermi National Accelerator Laboratory

FN-450
2023.000
2050.000

A Space-Time Analysis of Muo-Produced Hadronic Showers*

J.G. Morfín
Fermi National Accelerator Laboratory
P.O. Box 500, Batavia, Illinois 60510

February 1987

*Presented at the Workshop on Electronuclear Physics with Internal Targets, SLAC, Stanford, California, January 5-8, 1987.

Operated by Universities Research Association Inc. under contract with the United States Department of Energy

A SPACE-TIME ANALYSIS OF MUO-PRODUCED HADRONIC SHOWERS

Jorge G. Morfín
Fermi National Laboratory
Batavia, IL 60510

Abstract

Hadron showers, produced by high energy muons interacting on various targets, have been analysed for evidence of a space-time structure of parton fragmentation by the European Muon Collaboration. Target-dependent multiplicity ratios and Bose-Einstein interference phenomena both yield information on this subject.

Introduction

What I will be discussing in this presentation is the latest step in the process which has taken the concept of partons from being a theoretical explanation[1] for a surprising experimental result to a particle in its own right. While it is true that the unconfined parton has not yet been detected, the characteristics of the parton have been fairly well defined through experimentation[2]. By studying the space-time development of a high energy muo-produced hadron shower, we are trying to answer two more fundamental questions about the nature of the quark. First, **what is the quark-nucleon cross section?** Second, **when does the struck quark start fragmenting into hadrons?** Since the relevant distances and time intervals will turn out to be relatively large we will have opportunity to briefly look at the problem of quark confinement. Furthermore, we will see that a study of nuclear effects becomes not only very intriguing but crucial to answering the above two questions. As experimental references I will concentrate on the results of the European Muon Collaboration (EMC), which used muons of energy 100 - 300 GeV on various targets, and the Tevatron Muon Experiment[3] (TMC), scheduled to start running this spring at Fermi National Laboratory with 600 GeV muons. It is not coincidental that the primary goal of the TMC is a high statistics analysis of these nuclear effects.

Experimentally we are trying to determine **what happens between the time a muon is detected as entering the experimental target and a shower of hadrons emerges.** The process can be divided into three stages:

1. The muon transfers a fraction of its energy to a parton.
2. The parton travels through the nuclear medium and hadronizes.
3. The hadrons continue the passage through the target material and emerge.

Stage 1 covers such topics as the hadronic nature[4] of the photon which mediates the deep inelastic interactions (to be covered in these proceedings by T. Sloan) and the measurement of the nucleon structure function[5]. These results tell us the probability with which the photon will interact with a quark of a given flavor and what fraction of the total nucleon's momentum will be carried by the quark. Stage 3 has been studied for many years and is covered well by references[6] dealing with the passage of a particle through matter. Naturally stage 3 phenomena also includes hard final state scatters which would take us back to stage 2 ... etc.

Kinematics

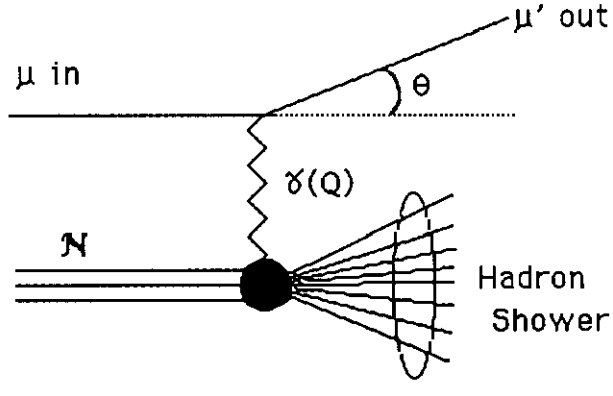

Fig 1. Feynman Graph representation of deep inelastic muon scattering

In discussing the phenomena of deep inelastic scattering, there are standard kinematic variables that are most helpful in characterising the interaction. If the incoming muon has energy E while the scattered muon has energy E' and scattering angle θ then the amount of 4-momentum transferred to the struck quark is:

$$Q^2 = 4EE'\sin^2 \theta/2 = -q^2$$

and the transferred energy is

$$\upsilon = E - E' .$$

The ratio of the 4-momentum transferred to the energy transferred is a measure of the fraction of the total nucleon momentum carried by the struck quark, as first formulated by Bjorken;

$$x_{Bj} = Q^2 / 2M\upsilon.$$

The hadronic shower is described by the effective mass of the shower

$$W^2 = M^2 + 2M\upsilon - Q^2,$$

and individual hadrons within the shower are characterized by the ratio of the hadron's energy to the total energy transferred to the hadron system

$$z = p / p_{max} = E_h / \upsilon.$$

Finally, Feynman-x relates a hadron's 3-momenta to the 3-momentum of the photon propagator, and the rapidity of a hadron is a measure of it's direction relative to the photon propagator's direction;

$$x_F = \frac{P_L^*}{(P_L^*)_{max}}$$

$$Y = 0.5 \ln \frac{E + P_L}{E - P_L}$$

Survey of Theoretical Ideas: A-Dependent Multiplicity Distributions

The significance of a space-time analysis of high energy processes as well as the basic ideas were summarized by Bjorken[7] in several fundamental reports from the mid 70's. He pointed out the importance of long time intervals and large distances which had been emphasized earlier by Landau and colleagues[8]. At the time, the emission of hard hadrons was postulated to be a tail effect of a bremsstrahlung-type process of soft hadron emission. In this case, the distance required for the hadron to form in the lab is simply the time/distance for the quark to fragment to the hadron in the quark rest frame - a distance of $\approx 1/m_h$ - boosted by its Lorentz factor (E_h / m_h) into the lab. This hypothesis was consistent with the observed[9] absence of intra-nuclear cascading of high energy hadrons since if E_h / m_h^2 > nuclear size, the hadron is formed outside of the nuclear matter.

A series of increasingly complex models followed these early concepts. They attempt to describe the behavior of leading hadrons with large z (or x_F):

Dar and Takagi[10] -- postulated that the leading quark either escapes completely or is entirely absorbed in a single interaction. With a quark-nucleon cross section (σ_{qN}) of 13 mb they were able to successfully describe the existing data as shown in Fig 2.

Nilsson, Andersson and Gustafson[11] -- The quark can interact more than once, transferring energy to a nucleon each time, before finally fragmenting. They needed a value of σ_{qN} = 20 mb to fit the data as in Fig 3.

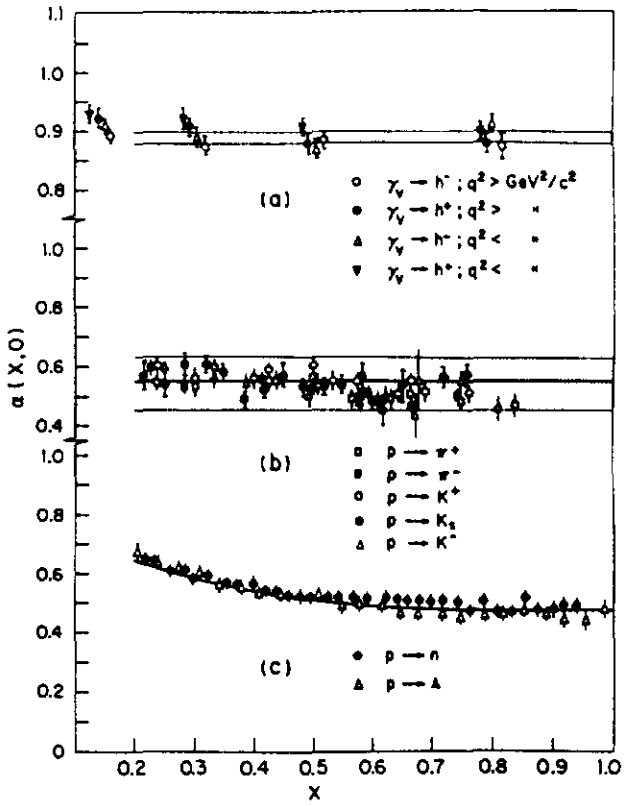

Fig. 2 The predictions of reference 10 (solid lines) compared to various experimental results.

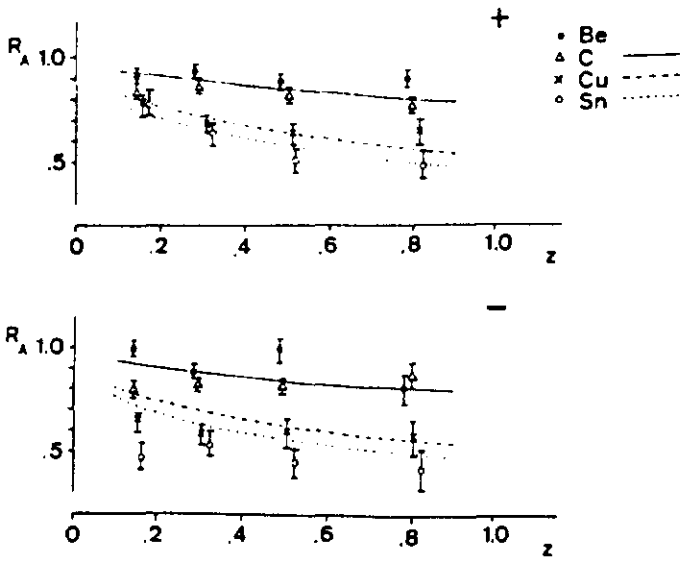

Fig. 3 The predictions of reference 11 compared to the positive and negative particles from the data of reference 17.

Bialas and Bialas[12] -- This model was relatively sophisticated in that it contained multiple elastic and inelastic quark - nucleon scattering. A separate analysis of the longitudinal and transverse hadron momentum spectra yielded information on σ_q^{inel} and σ_q^{tot} respectively.

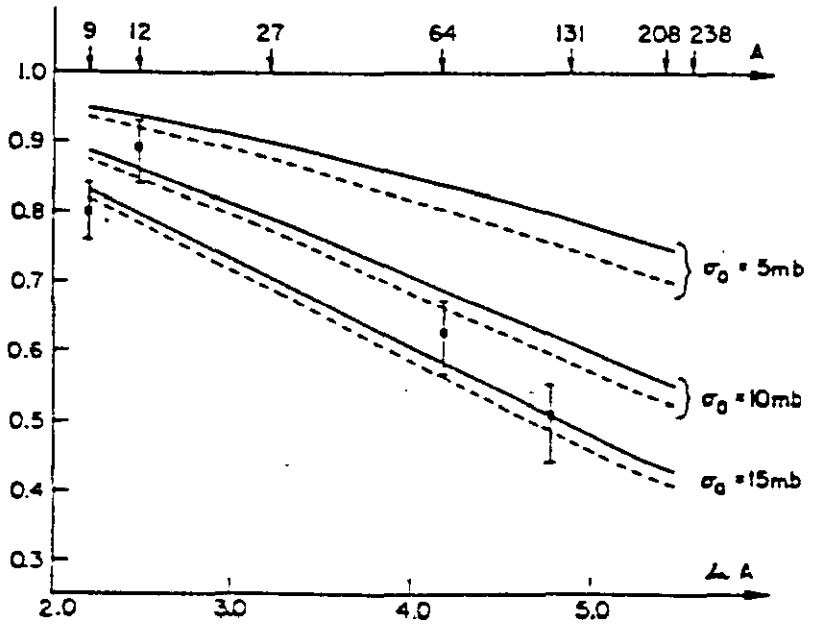

Fig. 4 The A-dependence of the ratio of hadronic yields from nuclei and H_2 for different values of the total quark-nucleon cross section. The data are from reference 17.

Bialas[13] -- This was the first model to stress the simple idea of measuring the A-dependence of the multiplicity of *different* leading hadrons. If it is the same, the intermediate state which escapes the nucleus is a quark. Bialas also stressed the importance of the interplay between σ_q and the formation length τ_q --> h.

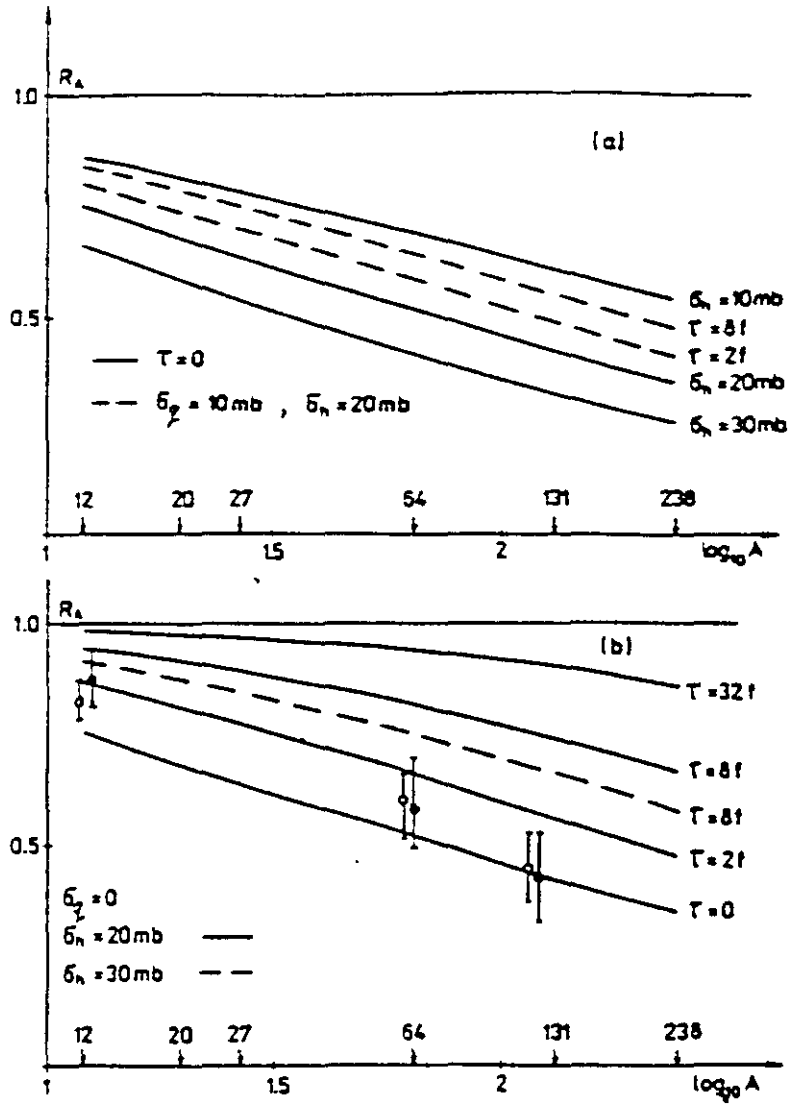

Fig. 5 The ratio of multiplicities from nucleus A versus H_2 for various values of the formation length and the quark nucleon cross section. The data are from reference 17.

Nikolaev[14] -- A very sophisticated model which uses a nuclear transport equation combined with the concept of formation length to predict multiplicity distributions for deep inelastic and photoproduced hadron showers.

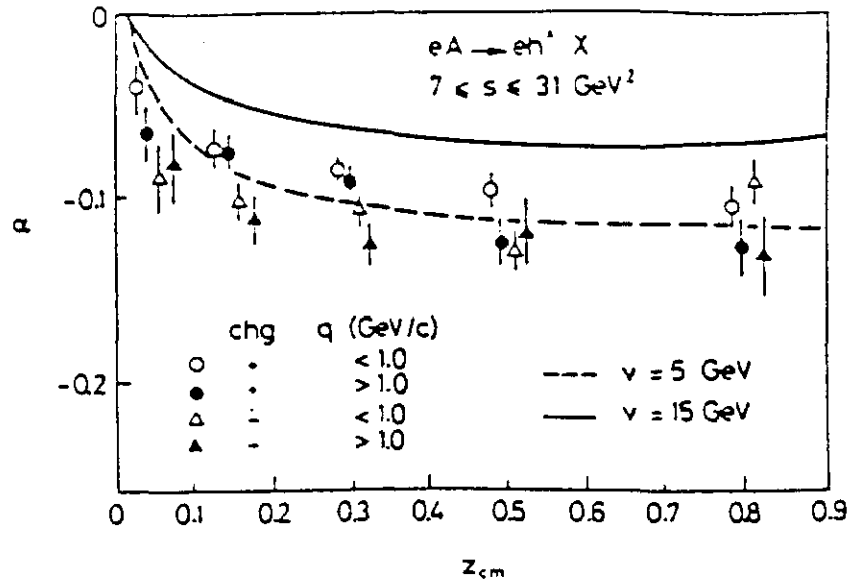

Fig. 6 The predicted behavior of α, the exponent of A^{α}, vs z in the cm system and compared to the data of reference 17.

Bialas and Chmaj[15] -- Introduced an alternative definition of formation length by postulating that fragmentation may be similar to the decay of the quark into a hard hadron. In this case, the formation length is $\tau = \upsilon / m_q^2$ where the quark life-time has been assumed to be $\approx 1 / m_q$.

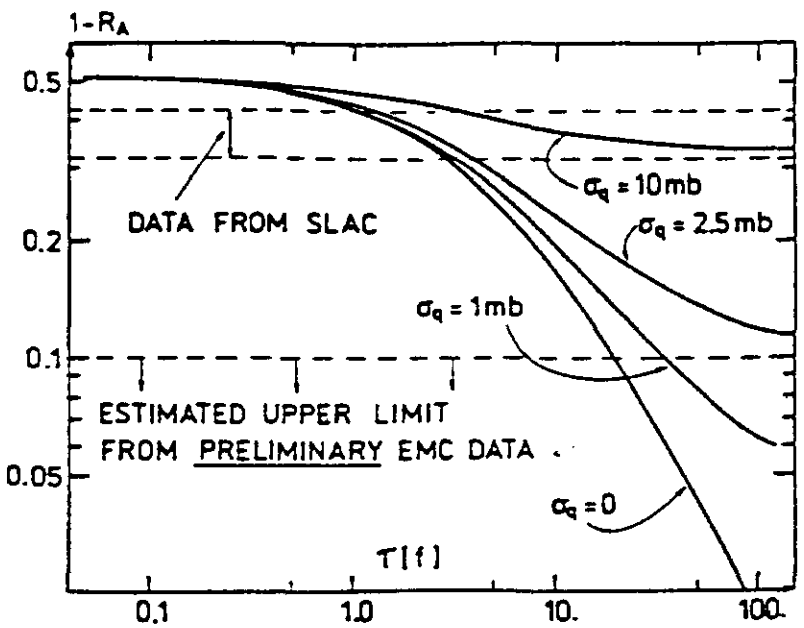

Fig. 7 The ratio of hadrons produced on copper and H_2 versus the formation length for various values of the quark nucleon cross section. The data are from reference 17 and early EMC results.

QCD Models[16] -- The application of QCD to the space-time development of hadron showers **does not appreciably change the basic scale invariant parton model predictions we have just outlined.**

Although we do seem to be suffering from an embaressment of riches in that all models seem to fit the available data, this will no doubt change when more experiments, over a wider energy range, can be included in the comparison. One common thread which binds all of the models which we have discussed and which has guided our planning of the Tevatron Muon Collaboration is that

To determine the validity of the various ideas contained in these models, a measurement of the A-DEPENDENCE of the hadron shower characteristics is crucial!!

Experimental Results: A-Dependent Multiplicity Distributions

The EMC experiment was not the first to study leptoproduced hadron showers. There have been electron and neutrino as well as earlier muon experiments which have studied lepton-nucleus scattering. However, the earlier experiments were handicapped by a lack of statistics and/or a low and limited energy range. Except for the SLAC results[17] using a 20.5 GeV electron beam with statistics of 10000 events per target, the earlier experiments were limited to 600 ($<E_\upsilon> \approx 20$ GeV) and 3100 ($<E_\upsilon> \approx 200$ GeV) event neutrino[18,19] experiments and an 88 event muon ($E_\mu = 150$ GeV) emulsion experiment[20].

The European Muon Collaboration, running without a vertex detector, took data with Carbon and Copper targets[21] and compared it with earlier data[22] using a hydrogen target. The main thrust of this phase of the experiment was to study the ratios of multiplicity distributions of hadrons produced off of these different nuclei. Examined was the ratio of differential multiplicity distributions

$$R_{A_1/A_2}(z) = \left(\frac{1}{N_\mu}\frac{dn}{dz}\right)_{A_1} / \left(\frac{1}{N_\mu}\frac{dn}{dz}\right)_{A_2}$$

and, to emphasize any nuclear effects on the leading hadrons, the ratio of integrated z distributions

$$\overline{R}_{A_1/A_2}(z_{min}) = \int_{z_{min}}^{1.0} dz \left(\frac{1}{N_\mu}\frac{dn}{dz}\right)_{A_1} / \int_{z_{min}}^{1.0} dz \left(\frac{1}{N_\mu}\frac{dn}{dz}\right)_{A_2}$$

Kinematic Cuts and Data Sample

To keep acceptance corrections small and consistent for the different nuclear runs, the following kinematic cuts were made on all samples;

$$Q^2 > 5.0 \text{ GeV}$$
$$\upsilon > 50.0 \text{ GeV}$$
$$x_{Bj} > 0.02$$
$$W^2 > 25.0 \text{ GeV}^2$$
$$P_{had} > 6.0 \text{ GeV} \quad .$$

After these cuts had been made, the following sample sizes were used in the final analysis:

Nucleus	E_μ	Events	$\langle W^2 \rangle$	$\langle \upsilon \rangle$	$\langle Q^2 \rangle$	$\langle x \rangle$
Hydrogen	120	9.0 K	121	71	12	.10
Hydrogen	280	9.8 K	174	108	29	.15
Carbon	200	13.9 K	186	110	21	.11
Copper	200	10.4 K	188	112	21	.11

The differences between the hydrogen and heavier nuclei samples arose since the Carbon and Copper runs were performed at a different time with a somewhat altered spectrometer.

Analysis

Since the analysis concentrates on the ratios of hadronic distributions from the three targets, it is the *differences* in the corrections which are crucial. For the acceptance corrections it was determined that at high z the acceptance during hydrogen running was twice as high as for the heavy nucleus runs. For the radiative corrections, the C and Cu data had to be corrected for coherent radiative processes in addition to the corrections which had been applied to the hydrogen sample. This amounted to, at most, a 5% correction to the Cu data in the lowest x range. The only other correction required to account for the difference between hydrogen and the heavier nuclei is a compensation for hadronic interactions with other nuclei of the target. Absorption or the creation of secondaries modified produced multiplicities. Using Monte Carlo techniques the maximum correction was found to be < 5%. **Note that after this correction the results correspond to zero target length.**

Results

The overall average multiplicities are 1.58 ± .02 for Carbon and 1.69 ±.02 for Copper. This represents an increase of 7% ± 2%(statistical) ± 3%(systematic) which is hardly significant. A more detailed look at the multiplicities is shown in Fig. 8. Even at this level there is no difference between the carbon and copper data.

To see if the multiplicities are dependent on the energy transferred to the struck parton, the data has been divided into three υ bins; 50 < υ < 70 GeV, 70 < υ < 90 GeV, and υ > 90 GeV. The results are shown in Fig. 9.

The average multiplicity ratios for leading (z>0.5) hadrons in the three υ bins is:

Ratio	50<υ<70	70<υ<90	υ>90 GeV
Cu/C	0.78±.13±.05	1.27±.20±.10	1.04±.12±.14
C/H_2	1.07±.13±.17	0.77±.12±.11	1.16±.12±.20
Cu/H_2	0.84±.12±.14	0.97±.14±.13	1.20±.12±.20

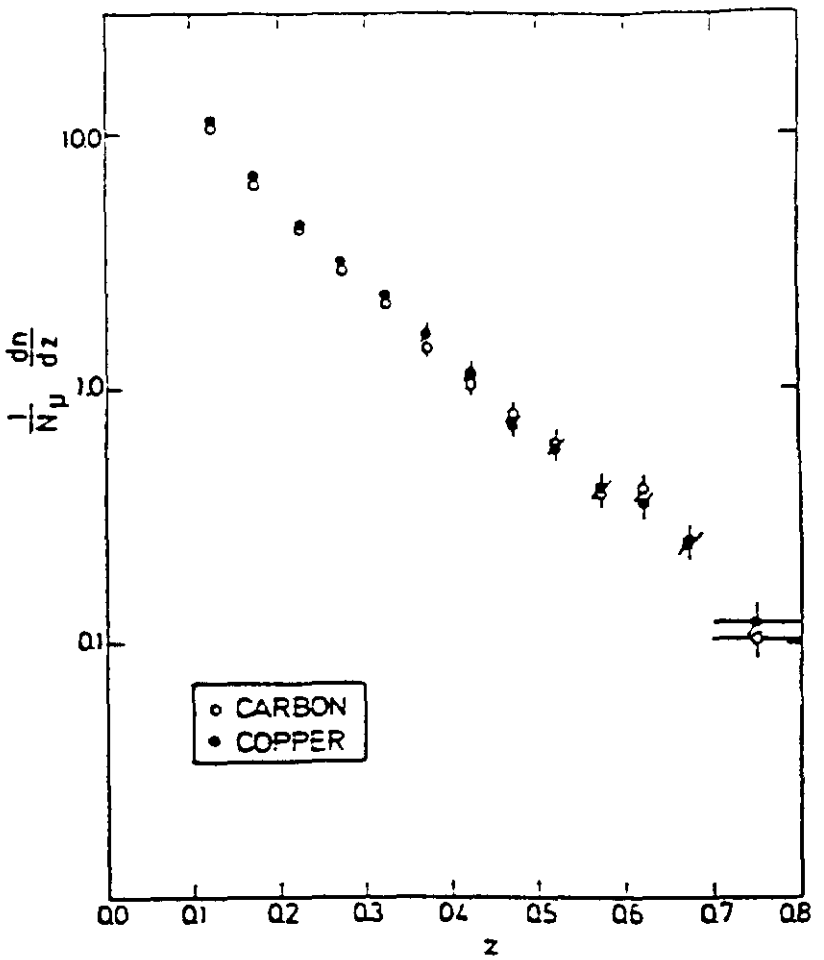

Fig. 8 Shows the charged hadron multiplicity as a function of z for C and Cu.

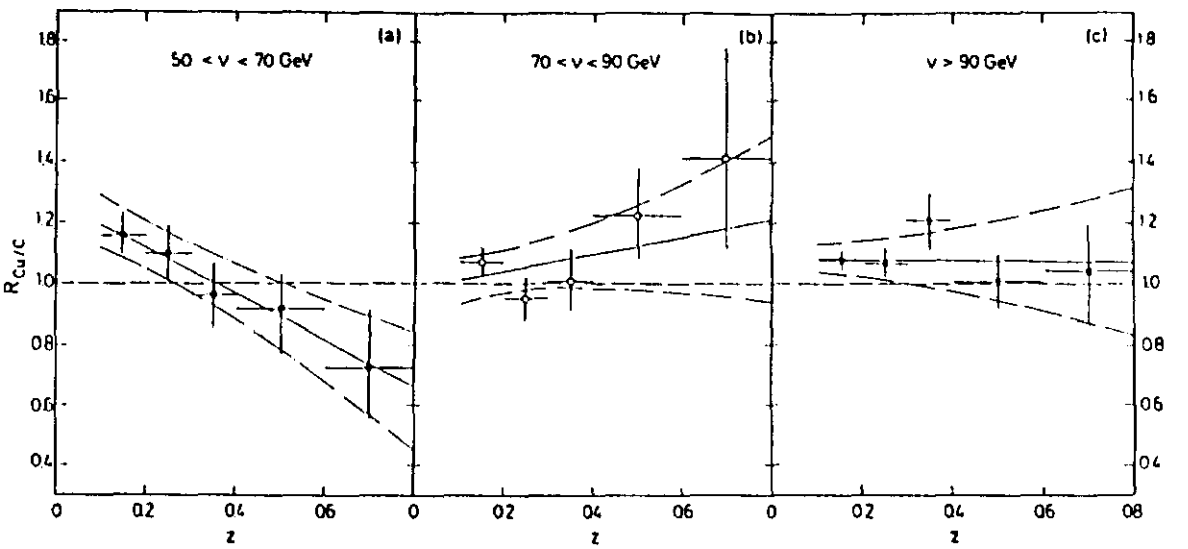

Fig. 9 The ratio of copper and carbon multiplicities as a function of z in three different virtual gamma energy bins. The solid lines are linear fits to the data and the dashed lines are the 1 sd limits.

The overall trend of the υ-dependence is a depletion of leading hadrons and an overall broadening of hadron showers at low υ in Cu compared to C and H_2.

There is a similar although statistically less significant effect when we look at the x_{Bj} dependence of the multiplicities. We find a depletion of leading hadrons and a broadening of the hadron showers at large x. Since $x = Q^2/2M\upsilon$ we are probably seeing a reflection of the previously mentioned υ dependence in the x-distribution.

We can combine these EMC results with the earlier SLAC[17] results for $3 < \upsilon < 17$ GeV.

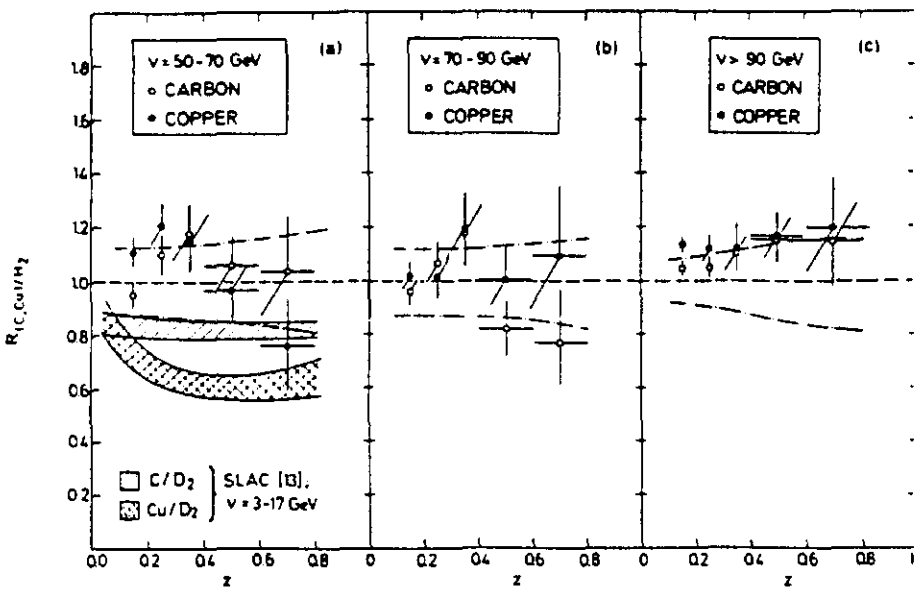

Fig. 10 The ratio of multiplicity distributions from EMC and the low energy SLAC results plotted together.

The nuclear effects are much more pronounced at the low SLAC values of υ. Assuming that the effect depends only on υ (not on Q^2), the model of Bialas[13] can be used to fit the two υ ranges (roughly $3 < \upsilon < 180$ GeV) of the SLAC and EMC results. Using the measured ratios of C:Cu <1.25 (2 s.d) by EMC at $\langle\upsilon\rangle \approx 100$ GeV and C:Cu > 1.17 by the SLAC group at $\langle\upsilon\rangle = 8$ GeV, and expressing the formation length τ as

$$\tau(\text{fm}) = \delta(\text{fm/GeV}) * \upsilon(\text{GeV})$$

then Fig. 11 shows the region in the δ-σ_{qN} plane allowed by the two results.

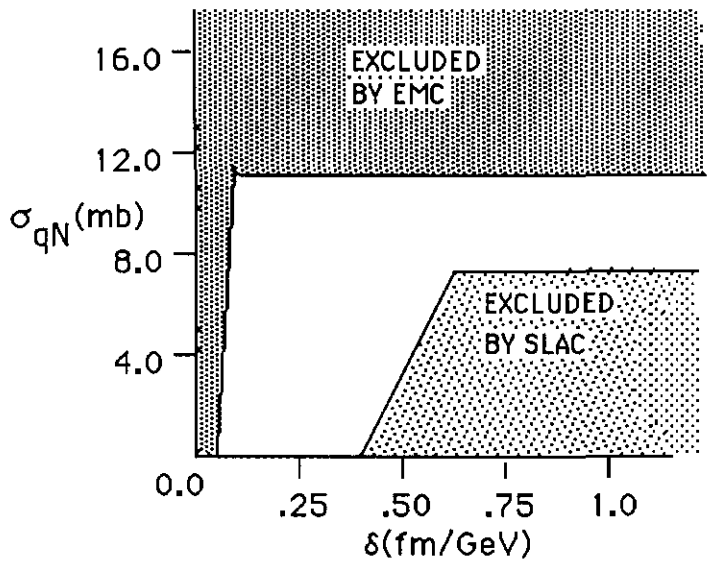

Fig. 11 Allowed region in the δ-σ_{qN} plane by both the SLAC and EMC results using the Bialas model.

It can be seen that the SLAC results favor smaller values of δ while the EMC results exclude $\delta = 0$. Cross sections larger than $\approx$ 10 mb are excluded by the EMC results. It should be quite obvious that much more exact data at all values of υ are necessary before further model dependent interpretation is possible.

Conclusions: A-Dependent Multiplicity Distributions

There is a depletion of leading particles and a broadening of hadron jets at low υ with increasing A of the target. Analysis of the EMC and SLAC results in terms of the Bialas model implies that τ, the formation length, is υ dependent and comparable to the size of the nucleus (r_C = 2.7 fm and r_{Cu} = 4.8 fm). Furthermore, the quark-nucleon cross section would have to be less than 10 mb to be consistent with the EMC results.

Improvements Expected from the Tevatron Muon Experiment

Following is a list of the major improvements we expect from the upcoming Tevatron experiment on nuclear targets compared to the recently completed EMC heavy target experiment:

1. Increase statistics by an order of magnitude
2. Improved acceptance for high-z particles.
3. Various A targets will be exposed in the same run to the same muon energy distribution resulting in reduced systematic errors.
4. There will be a factor > 2 larger kinematic range which should allow finer binning in υ and a measurement of the Q^2 dependence of the formation length τ.
5. Much better particle identification (i.e. K/π separation from 1 to 120 GeV) should improve the chance of measuring τ and σ_{qN} for different hadrons.

The Bose-Einstein Effect: Introduction

I am sure we all recall studying the difference between Fermi statistics and Bose-Einstein statistics in Quantum Mechanics and, perhaps, thinking that this will never apply to much that we would be doing professionally. This next method for studying the development of a hadron shower is a vindication of the hours invested in studying Bose-Einstein!

A method to use Bose-Einstein interference to determine the spatial extent of an object was first proposed by Hanbury-Brown and Twiss[23] in the mid 50's to determine the diameter of stellar objects using photon interferometry. Several years later, and unaware of the Hanbury-Brown Twiss work, G. Goldhaber and colleagues[24] noticed a distinct difference between the rate of like-charge and unlike-charge pion pairs as a function of the opening angle between the pions. After a month of contemplation they interpreted this result in terms of the Bose-Einstein effect for pions and were able to obtain a quantitative fit to their data by symmeterizing the two pion wave functions for like pions. In the intervening years the analysis has become much more sophisticated[25] and high statistics experiments now use correlation densities to extract the effect. Defining the one and two particle densities

$$\rho(p_1) = \frac{1}{\sigma}\frac{d\sigma}{dp_1}$$

$$\rho(p_1,p_2) = \frac{1}{\sigma}\frac{d^2\sigma}{dp_1 dp_2}$$

respectively, the two body correlation coefficient is given by

$$C_2 = \frac{\rho(p_1, p_2)}{\rho(p_1)\,\rho(p_2)}$$

To remove kinematic and dynamic correlations not associated with the Bose-Einstein effect, ratios are taken between a like-sign experimental density and a reference sample density which should not have any Bose-Einstein correlations,

$$R_0^{Like} = \frac{\rho(p_1, p_2)}{\rho_0(p_1, p_2)}$$

The quantity $(R_0{}^{Like} - 1)$ is the **Fourier transform of the space-time distribution of the particle source.**[26]

The important thing for experimentalists is that the consequences of the Bose-Einstein effect should be an enhancement of n(>1) identical boson final states compared to a final state composed of n dissimilar bosons. Using the parameterization chosen by the EMC collaboration[27], if $\Delta p = p_i - p_j$ is the difference of the 4-momenta of two like sign pions, then the ratio of like-sign pairs to non-interfering pairs can be expressed as

$$I = 1 + \lambda \exp(- \tilde{M}^2 R^2)$$

with $\tilde{M}^2 = -(\Delta p)^2$ the square of the difference of the pions 4-momenta and **R is the rms size of the pion source!** The factor λ is necessary to compensate for coherently produced pions.

The Bose-Einstein Effect: EMC Results

The European Muon Collaboration's full spectrometer (with streamer chamber and associated vertex detectors) was used to study the Bose-Einstein effect in muoproduced hadronic showers. Using 280 GeV muons on a H_2 target, a sample of events was collected which survived the following kinematic cuts;

$$Q^2 > 4 \text{ GeV}^2$$
$$4 < W < 20 \text{ GeV}$$
$$20 < \upsilon < 260 \text{ GeV}$$
$$y < 0.9$$
$$\theta_{\mu'} > 0.75^\circ \quad .$$

After further resolution associated cuts, the final sample consisted of 17,343 events.

Since only **50%** of the hadrons were identified, it was assumed that all negative hadrons were pions. This was justified by the Lund Monte Carlo results which showed that the ratio $\pi : K : P$ was 80 : 9 : 11. Furthermore, within the hadronic shower all particles had to have momentum measurements with $\Delta P/P < 20\%$ and, most significantly, all accepted tracks had to be measurable in the streamer chamber. This last requirement effectively limited the particles to $x_F < 0.2$ which is relatively low momentum particles. Under these conditions the following combinations were found

126,000 $(\pi^+\pi^-)$ combinations

60,000 $(\pi^+\pi^+)$ combinations
38,300 $(\pi^-\pi^-)$ combinations
98,300 like sign pion pairs

Results

The most difficult task in the analysis is separating the Bose-Einstein Effect from elementary kinematic and dynamic correlations. The standard technique, mentioned above, is to form ratios of the like-sign pairs--$\rho(p_1,p_2)$--to pairs where the Bose-Einstein effect should be absent--$\rho_0(p_1,p_2)$. In the EMC analysis three reference groups

were formed:

REF 1	$(\pi^+\pi^-)$ combinations from the same event in which a like-sign pair was found,
REF 2	$(\pi^+\pi^-)$ combinations from the same event but with transverse momentum from random pions within the event,
REF 3	LIKE combinations constructed from random tracks from various events.

The LIKE/REF ratios as a function of $\tilde{M}^2$ are shown in Fig. 12a. There is the expected increase in the ratio as $\tilde{M}^2$ approaches 0, but there is an inconsistency in the shapes as well as the overall normalization of the three curves. This is an indication that there are still dynamical or kinematical correlations that remain uncompensated in the ratios. The next step in eliminating these non-interfering correlations involves the use of the Lund Monte Carlo[28] which does <u>not</u> contain Bose-Einstein interference effects. Subjecting the Monte Carlo events to the same cuts as the data the ratio LIKEMC/REFMC is formed. Again it is seen--Fig. 12b--that there is a disagreement in shape and normalization between the three ratios which can arise only from residual dynamic and/or kinematic correlations inherent in the LIKE sample. Since the LIKE/REF ratios contain a mixture of Bose-Einstein interference plus residual correlations, and the LIKEMC/REFMC ratios contain only the residual correlations, then the "ratio of ratios" (LIKE/REF) / (LIKEMC/REFMC) should reflect the sought after Bose-Einstein effect!

The results -Fig. 12c- now show a trend which is similar in both shape and magnitude indicating that the non-interfering correlations have been more successfully removed. A fit to $\tilde{M}^2$ and λ yields the following values, using the double ratios, for the three reference samples

	R(fm)	λ	χ^2 (ndf = 12)
REF 1	0.84 ± 0.03	1.08 ± 0.10	12.4
REF 2	0.66 ± 0.01	0.60 ± 0.06	12.2
REF 3	0.46 ± 0.03	0.73 ± 0.06	20.3

The results still depend on the reference sample which indicates that there are some correlations that have not been removed from the LIKE sample. Berger and his colleagues have shown[29] how intertwined the Bose-Einstein and resonance correlations can be.

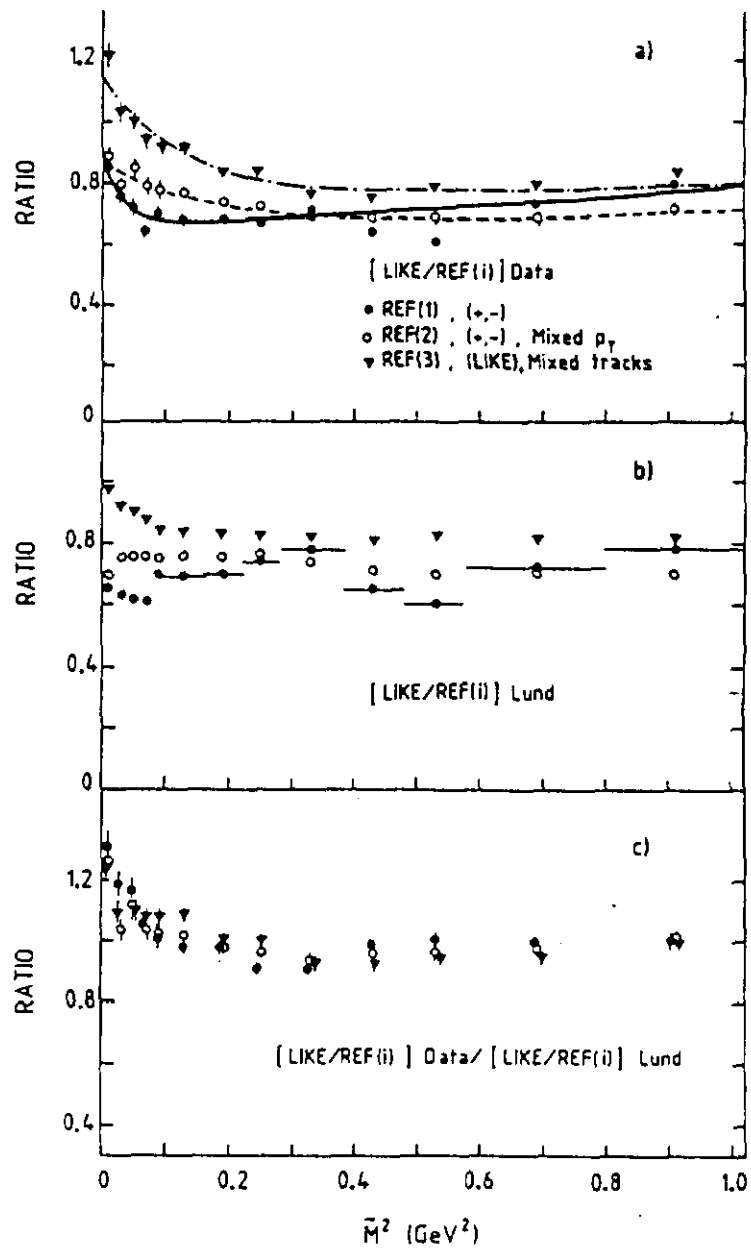

Fig. 12 Ratios as a function of the difference in the 4-momenta of the pion pairs. a) ratio of LIKE to REF(i) as defined above, b) the same ratios when using the Lund Monte Carlo results and c) the ratio of ratios a) and b).

Conclusion

The EMC analysis continues in an attempt to extract the shape of the pion emission region and the details can be found in reference 27. The EMC group comes to the conclusions that;

1. The Bose-Einstein interference effect has been seen in muoproduced like-sign pion pairs,
2. The results are consistent with a **spherically** shaped pion emission region, and
3. The radius of the emission region is **$0.46 < R < 0.84$ fm** and the suppression factor is $0.6 < \lambda < 1.0$.

These results are approximately consistent with almost every other experiment, regardless of energy or target, which has attempted the analysis. This, as well as the *spherical* nature of the emission region, tends to go against intuition and might indicate that there is something not consistent with either the method and/or the interpretation of the results of the Bose-Einstein analysis.

Critique

No one doubts the validity of Bose-Einstein statistics so that there should indeed be an interference effect that would enhance the number of "similar" bosons. However, aside from the difficulty of extracting the signal due to interference from the non-interfering correlations, the question of interpretation of the result is quite crucial.

The method used by the EMC and others, which involves describing the pion emission region with a single spatial variable R, is realistic in only a very few situations[30]. There is obviously no directional information in R so the data can only be described by this form if the source density of the emission region depends only on the length of the 4-vector difference between the two pions. Furthermore, and most telling, the 4-momentum difference of any pair of pions as well as the "shape" of the source has to depend on the frame in which they are being evaluated. Fig. 13 illustrates this by indicating a pair of pions which have identical 4-vectors in a frame where the current and target fragment sources are moving in opposite directions with respect to each other. Upon boosting to the lab they are no longer "identical pions". This, of course, implies that if lab momenta are used to search for identical

pion pairs, there is no way that the resulting pion source size can be a measure of the **total emission (current + target fragments) region!** It is, at best, a measure of the spatial extent of <u>either</u> current fragment sources or target fragment sources. Even this interpretation is not necessarily correct if there is an ordered momentum/space-time correlation, as postulated by Bjorken and incorporated by the successful Lund Monte Carlo, so that particles with similar momentum have been emitted at **neighboring** space-time points in the evolution of the hadronic shower!

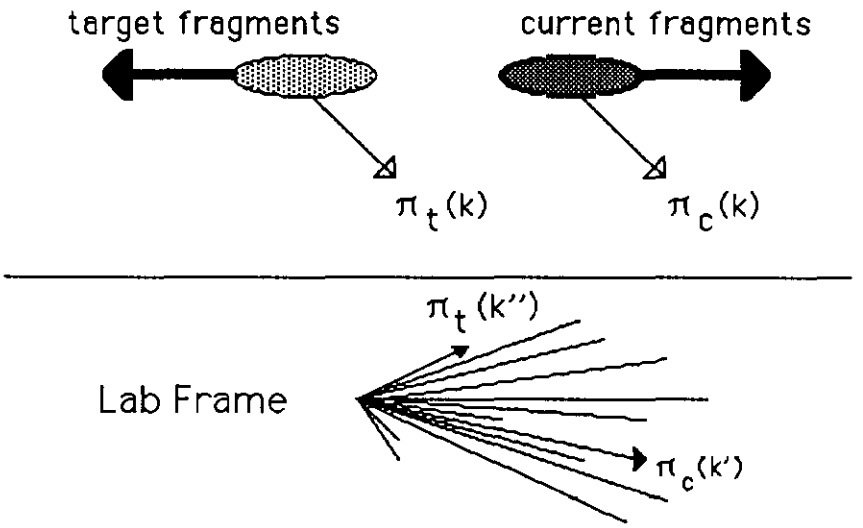

Fig. 13 Identical pion in one frame are not identical pions in all frames.

There have been attempts[30,31], particularly in the interpretation of e^+e^- Bose-Einstein analyses, to determine whether currently acceptable hadronization models, such as the Lund-type string model, might yield the results found by almost all Bose-Einstein analyses including the EMC result. Both of the references find consistency between string model predictions and the experimental results that the emission region is "spherical" and the associated length is of the order of 1 fm. <u>However, this length has little to do with the spatial extent of the source of all particles in the shower.</u>

The TMC will take a much more critical look at the method and

interpretation of Bose-Einstein interference effects. Much improved particle identification, improved momentum resolution and increased kinematical range should allow Bose-Einstein analyses in more than one reference frame and off various targets.

Overall Conclusion

The topic of the space-time development of a hadron shower, although of fundamental importance, has barely progressed beyond the most elementary level of experimental investigation. The concepts of quark-nucleon cross sections and hadron formation lengths are still more philosophical than scientific quantities. There is a need for carefully controlled, high statistics measurements of hadron multiplicities off a variety of nuclear targets and over a wide kinematic range before a quantified knowledge of the space-time structure of a hadronic shower can be claimed. This need will be answered by the upcoming Tevatron Muon Collaboration which will begin taking data at Fermilab in the very near future. A second experiment, preferably covering lower energies than this Tevatron experiment, would be extremely useful in answering the questions posed in this presentation.

Acknowledgements

I would like to thank Ray Arnold and Karl Van Bibber for their kind hospitality and the opportunity to view this fascinating physics from both ends of the energy scale. My thanks also to J. D. Bjorken for helpful comments and clarifications.

References

1. R. P. Feynman, Photon-Hadron Interactions, W. A. Benjamin, New York, 1972.
2. T. Sloan, Recent Results in Deep Inelastic Scattering, CERN EP/86-111, August, 1986.
3. Muon Scattering with Hadron Detection at the Tevatron, Fermilab Experiment 665.
4. T. Sloan, Recent Results in Deep Inelastic Scattering, CERN EP/86-111, August, 1986.

5. J. J. Aubert et al., Nucl. Phys B272 , 158 (1979).
6. E. Segre, Nuclei and Particles, W. A. Benjamin, New York, 1964.
7. J. D. Bjorken, SLAC-PUB-1756, May 1976.
8. L. D. Landau, Izv. Acad. Nauk. SSSR 17, 31 (1953).
9. W. Busza, Acta Phys. Pol. B8 , 333 (1977).
10. A. Dar and F. Takagi, Phys. Rev. Lett. 44, 768 (1980).
11. G. Nilsson, B. Andersson and G. Gustafson, Phys. Lett. 83B, 379 (1979).
12. A. Bialas and E. Bialas, Phys. Rev. D21, 675 (1980).
13. A. Bialas, Acta Phys. Pol. B11, 475 (1980).
14. N. N. Nikolaev, Z. Phys. C 5, 291 (1980).
15. A. Bialas and T. Chmaj, Phys. Lett. 133B, 241 (1983).
16. S. J. Brodsky, SLAC-PUB-2970, September 1982.
A. H. Mueller, Topics in High Energy Perturbative QCD Including Interactions with Nuclear Matter, Proc. XVIIth Rencontre de Moriond, Les Arcs, 1982.
17. L. S. Osborne et al., Phys. Rev. Lett. 40, 1624 (1978).
18. J. P. Berge et al., Phys. Rev. D18, 3905 (1978).
19. H. Deden et al., Nucl. Phys. 198B, 365 (1982).
20. L. Hand et al., Z. Phys. C 1, 139 (1979).
21. A. Arvidson et al., Nucl. Phys. B246, 381 (1984).
22. J. J. Aubert et al., Phys. Lett. 114B, 373 (1982).
23. R. Hanbury-Brown and R. Q. Twiss, Philos. Mag. 45, 663 (1954).
24. G. Goldhaber et al., Phys. Rev. Lett. 3, 181 (1959).
25. G. Goldhaber, LBL Preprint 19417 (1985).
26. G. Goldhaber et al., Phys. Rev. 120, 300 (1960).
27. M. Arneodo et al., CERN-EP/86-42, April 1986.
28. G. Ingelman et al., Nucl. Phys. B206, 239 (1982).
29. E. L. Berger et al., Phys. Rev. D15, 206 (1977).
30. M. G. Bowler, Z. Phys. C 29, 617 (1985).
31. B. Andersson and W. Hofmann, Phys. Lett. 169B, (1986).